A finite element analysis for unbonded flexible risers under bending loads

Chen Xiqia[*1], Fu Shixiao[2], Gao Yun[3] and Du Xiaying[1]

[1]*Tianjin Branch, CNOOC Ltd, Tianjin, China*
[2]*State Key Laboratory of Ocean Engineering, Shanghai Jiao Tong University, Shanghai, China*
[3]*State Key Laboratory of Oil and Gas Reservoir Geology and Exploration,
Southwest Petroleum University, Chengdu, China*

Abstract. As the exploitation of oil and gas resources advances into deeper waters and harsher environments, the design and analysis of the flexible risers has become the research focus in the offshore engineering filed. Due to the complexity of the components and the sliding between the adjacent layers, the bending response of the flexible risers is highly non-linear. This paper presents the finite element analysis of the flexible risers under bending loads. The detailed finite element model of the flexible riser is established in ABAQUS software. This finite element model incorporates all the fine details of the riser to accurately predict its nonlinear structural behavior. Based on the finite element model, the bending moment–curvature relationships of a flexible riser under various axisymmetric loads have been investigated. The results have been compared with the analytical ones obtained from the literature and good agreements have been found. Moreover, the stress of the tendon armors has been studied. The non-linear relationship between the armor tendons' stress and the bending loads has been obtained.

Keywords: flexible risers; finite element model; non-linear; bending loads; axisymmetric loads; stress

1. Introduction

As the exploitation of oil and gas resources advances into deeper waters and harsher environments, flexible risers are widely used (Do 2011, Huang *et al*. 2013, Eom *et al*. 2014, Ren 2014). The main advantage of flexible risers is that they are compliant and highly deformable in bending, while maintaining sufficient tensile stiffness to withstand large deformations induced by self weight, currents, waves, vortex-induced vibrations, and motions of the floating vessels (Song 2013). However, due to the complexity of the structural form, the design and analysis of flexible risers is a complex topic.

Regarding the complicacy and importance of the bending responses of unbounded flexible risers, lots of researches have been done in this field in last 15 years. Among analytical studies, Dong *et al*. (2013) conducted thorough studies on this topic. A straightforward analytical model was developed based on the Coulomb friction model and the principle of virtual work. Their model had considered the nonlinearity caused by sliding of individual helical tendons between the

∗Corresponding author, E-mail: chenxq33@cnooc.com.cn

surrounding layers. The significant impact of interlayer contact pressure on the moment–curvature relationships was illustrated in their case study. Meanwhile, the impact of local bending and twisting of tendons on the bending stiffness of flexible risers was analyzed. According to their analysis, the local bending and twisting of helical tendons on the bending behavior for the entire riser was significant under the full-slip state.

Among the numerical studies, Bahtui *et al*. (2008a, b) studied the response of a five-layer flexible riser under axisymmetric loads with a detailed 3D finite-element model using the ABAQUS software. In this model, all layers were represented by 3D solid elements and contact elements, with friction properties were defined between each contact pair of layers. Alfano *et al*. (2009) proposed a constitutive model for flexible risers, which could be efficiently used for large-scale analyses. The constitutive model was formulated by the framework of an Euler-Bernoulli beam model, with the addition of pressure terms to account for the internal and external pressures. The proposed model had been validated by a very detailed no-linear finite element model. Bahtui *et al*. (2010) also conducted multi-scale analysis of the un-bonded flexible risers. In the analysis, the constitutive law for un-bonded flexible risers was proposed and the multi-scale approach for the identification of the related input parameters was developed. Merino *et al*. (2010) analyzed the response of flexible pipes under torsion with a three-dimensional nonlinear finite element model. The estimations of the finite element model had agreed quite well with the experimental data performed at COOPPE/UFRJ. Saevik and Bruaseth (2005) presented a finite-element model for predicting the structural behavior of umbilical cables under axisymmetric loads by combining the curved-beam kinematics, thin-shell theory, and the principle of virtual displacement. The model considered a number of nonlinear features such as material nonlinearities, gaps between individual bodies, and hoop response due to contact effects. Later, Saevik and Gjosteen (2012) introduced bending analysis into this model.

The finite element analysis presented in this paper can provide an accurate approach to simulate the bending structural behavior of flexible risers. A highly detailed finite-element model has been developed, in which all the fine details of the flexible riser are considered. All layers of the flexible riser are modeled separately, contact interaction and friction between layers has been considered. Based on the developed model, the bending moment–curvature relationships of a flexible riser under various axisymmetric loads have been investigated. Moreover, the stress of the tendon armors has also been studied.

2. Pressure armor representations

The pressure armor is made by a metallic ribbon with a typical profile conformed to a helical shape, as shown in Fig. 1. Without any simplifications, the finite element model of the pressure amore would have a high number of degrees freedoms. Thus, de Sousa et al. (2009), proposed an alternative approach, in which the pressure armors are represented as orthotropic shells. The main idea of this approach is to assure that both the pressure armor and the orthotropic shell have the same stiffness.

The stiffness equivalence leads to the thickness, h_s, Young modulus, E_{s_x}, and the shear modulus of elasticity, $G_{s_{xy}}$, for the orthotropic shell given by the following expressions

Fig. 1 Typical geometry of the interlocked pressure armor

$$h_s = \sqrt{\frac{12 \cdot I_{eq}}{A}} \; , \quad E_{s_x} = \left(\frac{n_t \cdot A}{L_p \cdot h_s}\right) \cdot E, \quad G_{s_{xy}} = \left(\frac{3 \cdot n_t \cdot J}{L_p \cdot h_s^3}\right) \cdot G$$

(1)

where E and G are the Young and shear modulus of the material that constitute the tendon; n_t is the number of tendons in the considered layer, which is, generally, 1 or 2; A and J are cross-sectional and the torsional constant of the tendon; L_p is the pitch of the tendon, it can be expressed as

$$L_p = \frac{2 \cdot \pi \cdot R}{\tan \alpha}$$

(2)

in which R is the mean radius of the layer and α is the lay angle of the tendon. I_{eq} is given by

$$I_{eq} = 12 \cdot n_t \cdot \frac{I_y^2}{L_p} \cdot \frac{1 - v^2}{h^3}$$

(3)

where v is the Poisson ratio of the material that constitutes the tendon; h is its height; and I_y is the lower second moment of the area of the wire.

3. Finite element model

Bahtui *et al*. (2008a, b) has presented a numerical modeling procedure for unbounded flexible risers in ABAQUS software. Based on the procedure, the finite element model of an 8'' flexible riser consisted of 7 separate layers has been developed. Fig. 2 presents a general view of the numerical model of the unbonded flexible riser. In the model, all the layers except the pressure armor layer are presented in a realistic way. The pressure armor layer is simplified to reduce our numerical work.
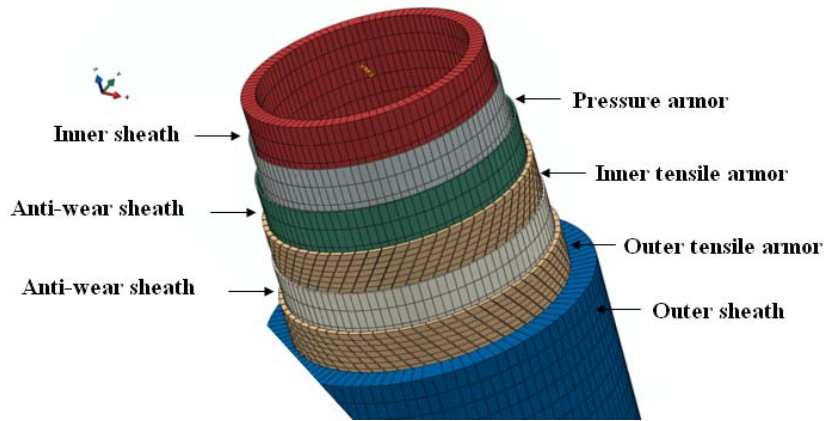
Fig. 2 The view of the numerical model

Element selection: The model is established using the ABAQUS software. The elements used in the model are of eight node linear brick type with integration and hourglass control for the sheath, anti-wear and tensile armor layers. Meanwhile, four-node doubly curved thin shell type with reduced integration and hourglass control is used to simulate the pressure armor layer. The integration along the shell thickness is applied by Simpson's integration technique. The number of section points through the thickness of the shell is 5, integrated during all iterations of the analysis.

The finite element analysis conducted in this paper is highly nonlinear due to the presence of contact surfaces as well as the large displacements taking place in the tendons of the helical armor layer. Thus, the above elements are chosen to well model the large displacement effects.

Contact definition: 3D contact elements are defined in the model for predicting the contact interaction between the layers during all stages of the loading. The contact analysis applies a penalty method based on Coulomb friction model together with the general contact algorithm of ABAQUS/Explict.

Meshing: Each layer of the model is meshed separately in ABAQUS. The element size of each layer should be defined appropriately to ensure the adjacent layers contact in a right way. Using few elements in the circumferential direction for different layers may lead to initial penetration in the radial direction. Layer penetration may result in initial radial acceleration produced by contact algorithm. Therefore, mesh convergence should be fully studied.

Solver selection: The dynamic explicit solver of ABAQUS is used due to the large number of contact surfaces. In the explicit analysis, loading should be applied at a sufficiently low rate to ensure that the analysis remains steady, avoiding any significant vibration. The low loading rate requires a small time increment, which depends on the modulus of elasticity, the density, and the element size. For the analysis presented in this paper, it is validated that a value of $\Delta t = 2 \times 10^{-7}$ sec is small enough to ensure the steadiness of the time-history analysis.

Besides, the hourglassing is monitored carefully through the analysis by keeping the ratio of hourglass energy to internal energy well below 5%.

4. Case studies

Based on the above finite element model procedure, the structural response of the flexible riser under bending load is studied. Detailed parameters on the flexible riser are listed in Table 1. Based on Eq. (1), the equivalent thickness and Young modulus of the pressure armor are calculated and listed in Table 2.

The length of the finite element model is 1.8 m, which is approximately 1.5 pitches of the tendon armors. This model contains 89008 elements and 247450 nodes. The coefficient of friction between all layers is assumed to be 0.1, as given in experimental results Saevik and Berge (1995)

As shown in Fig. 3, all the nodes at each of the two cross sections at both ends of the riser are rigidly connected to two reference points which are positioned at the centre of the sections. All boundary conditions for both ends are applied to these two reference points only. All loads (such as tension and bending) are applied to the references point at the top end of the riser only.

The sliding of individual helical tendons against their surrounding layers is the main reason for the nonlinearity behavior of the flexible riser under bending loads (Dong *et al*. 2013). In order to study the bending behavior carefully, the slip initiation and progression of the helical tendons are simulated in the finite element model.

In this finite-element model, the interlayer contact pressure is introduced from axisymmetric loads. Hence, the load cases considered in this paper are defined as bending with tension and bending with different internal and external pressures, referred to case 1, 2, and 3. Internal pressure is applied on the inner face of the innermost layer, and the external pressure is applied on the outer surface of the outermost layer. All the loads cases include two load steps: an initial loading (tension or internal and external pressures), and the bending loading. The two load steps are set to be 0.1 s and 1 s, respectively. All loads are applied as a linear function of the time in each step. All the load cases are listed in Table 3.

5. Results and discussion

Based on the developed finite element model, the bending responses of the flexible riser under the three load cases are analyzed. The dispalcements and von mises stresses for the tendon layers under load case 2 are shown in Figs. 4(a)-4(c).
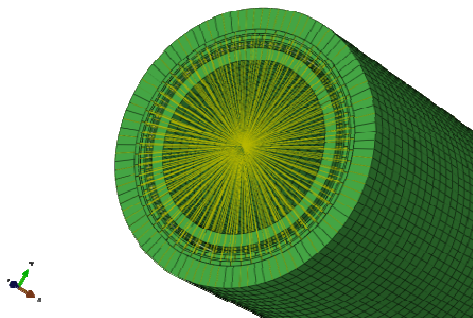

Fig. 3 The connection of the reference point
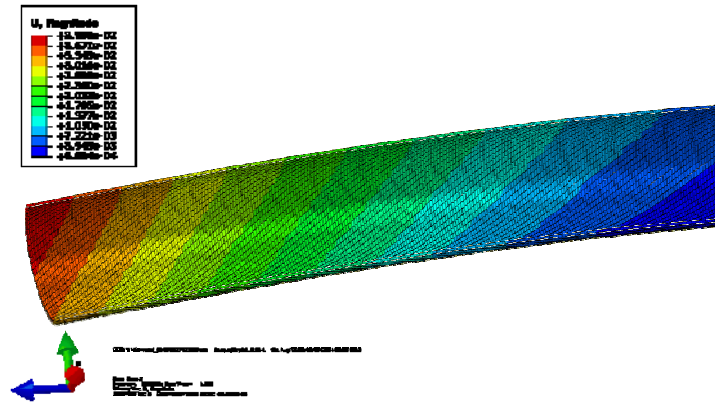
Table 1 Detailed information of the 8''flexible riser

Layer (material)	Properties
Inner sheath (HDPE)	Thickness=12 mm, Young modulus=600MPa, Poisson ratio=0.4
Pressure armor (Carbon steel)	Thickness=10 mm, number of wires=1, Lay angle=+89° Z profile area=91.7 mm^2, Moment of inertia=308 mm^4 Young modulus=210GPa, Poisson ratio=0.3
Anti-wear tape (PA11)	Thickness=2 mm, Young modulus=600MPa, Poisson ratio=0.47
Inner tensile armor (Carbon steel)	Thickness=4 mm, Number of wires=63, Lay angle=+35° Rectangular profile width：8mm, Young modulus=210GPa Poisson ratio=0.3
Anti-wear tape (PA11)	Thickness=2 mm, Young modulus=600MPa, Poisson ratio=0.47
Outer tensile armor (Carbon steel)	Thickness=4 mm, Number of wires=66, Lay angle=-35° Rectangular profile width：8 mm, Young modulus=210GPa Poisson ratio=0.3
Outer sheath (HDPE)	Thickness=22 mm, Young modulus=600MPa, Poisson ratio=0.4

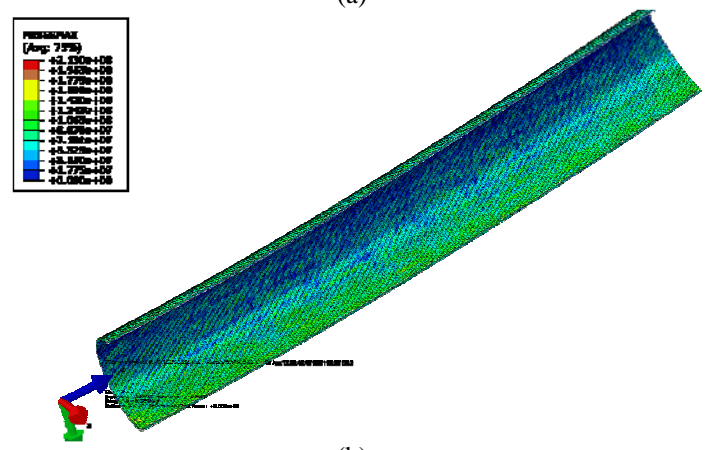Table 2 Equivalent parameters of the pressure armor

Thickness	Young modulus
6.34 mm	165GPa

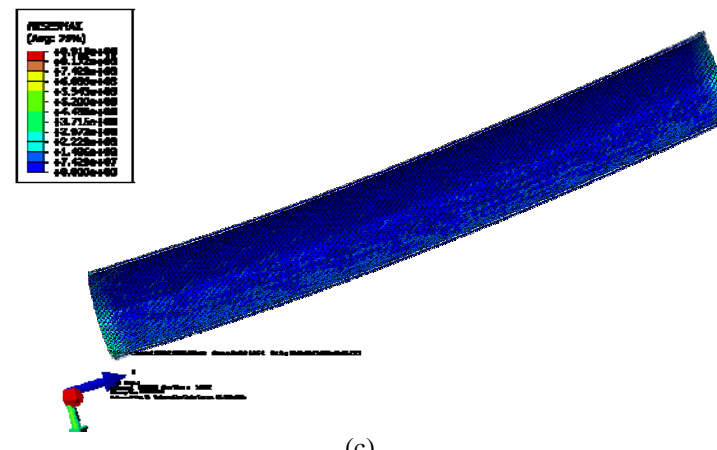Table 3 Load cases: steps and values

Case	Step 1	Step 2
1	Tension=600 kN	Bending moment=20kN．m
2	Internal pressure=5MPa External pressure=3MPa	Bending moment=20kN．m
3	Internal pressure=8MPa External pressure=6MPa	Bending moment=20kN．m

(a)

(b)

(c)

Fig. 4 (a) The dispalcement contour for the inner tendon layer under load case 2 (b) The Mises stress contour for the inner tendon layer without boundary parts under load case 2 (c) The Mises stress contour for the inner tendon layer with boundary parts under load case 2

Fig. 4(b) corresponds to load case 2 and shows the von Mises stress contour. As shown in the Figure, the von Mises stress of the inner tendon layer near the riser bending neutral axis is the minimum, however that farthest away from the riser bending neutral axis is the maximum. This stress distribution agrees well with the deduction in (Dong *et al.* 2013). When comparing the stress contours in Figs. 4(b) and 4(c), the stress at extremities of the model is extremely lager, this fact is because all the boundaries and loads are applied to the two extremities of the model, which causes the stress concentration. Hence, the stress analysis should neglect the boundary effect.

5.1 Bending moment–curvature results

To demonstrate the accuracy and stability, the bending moment–curvature results of the finite element model are compared with the analytical ones calculated based on the models presented in (Dong *et al.* 2013).

Figs. 5 and 6 show the relationship between the bending moment and the curvature under load cases 1 and 2. The results from the finite element analysis have satisfactory agreements with the analytical ones. The bending behavior is highly nonlinear because of the significant sliding.

As shown in Fig. 7, the distance 'a' between the two tendons in inner and outer tension layers has decreased to 'b' as the flexible risers bends. This fact visually validates the slippage that occurs between the tension layers.

Analyzing the slopes of two lines in Figure 6, the analytical results can be divided into three parts: curvatures smaller than the minimum critical curvature (curvature ranges from 0 to 0.0023/m), curvatures between the minimum and the maximum critical curvatures (curvature ranges from 0.0023/m to 0.0043/m), and curvature greater than the maximum critical curvature (curvature ranges from 0.0043/m to 0.036/m). The bending stiffness of the riser remains constant at the first and the third parts, and the stiffness at the second part decrease from the value at the first part to that at the third part. Compared with the analytical results, the bending stiffness of the finite element results varies much more gradually. This can be explained by the fact that the finite element model gradually takes into account of the effect of sliding of the armor tendons.
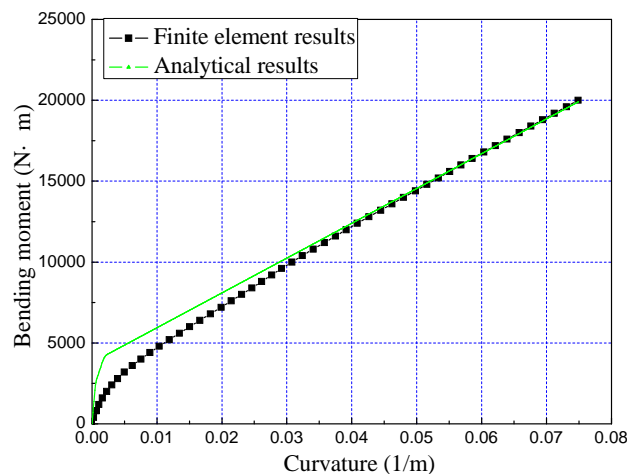

Fig. 5 Bending moment–curvature relationship of the flexible riser under load case 1
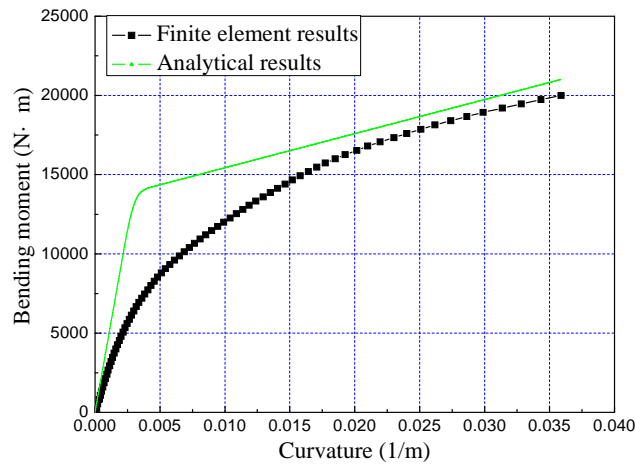
Fig. 6 Bending moment–curvature relationship of the flexible riser under load case 2

Fig. 7 Slipping of the tendon armors under load case 2

The bending moment–curvature relationships of the flexible riser under different pressure is shown in Figure 8. It is apparent that noticeable variation in the bending response of the flexible riser appears when the pressure changes. With an increase in the pressure, the bending curvature range under the no-sliding state increases correspondingly. It is caused by the fact that the larger amount of pressure causes the higher interlayer contact pressure, leading to a greater critical curvature.
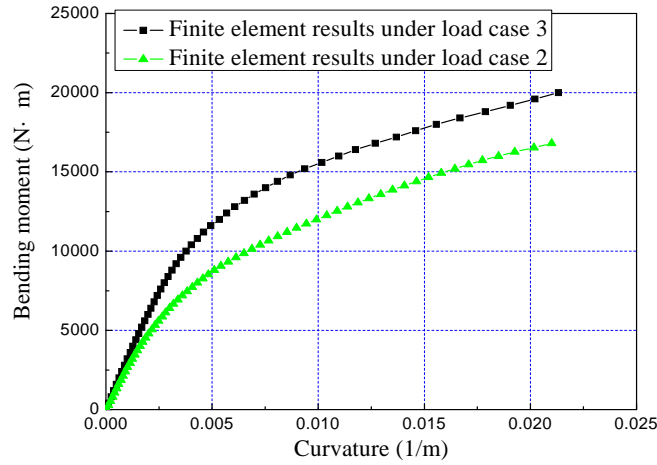
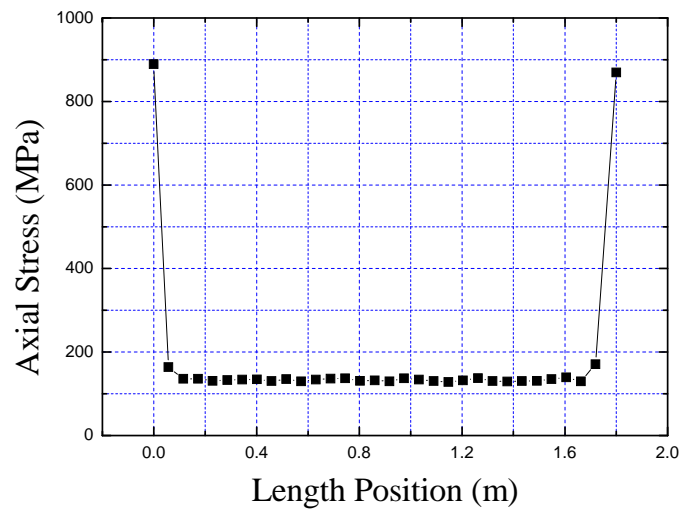Fig. 8 Bending moment–curvature relationship of the flexible riser under load cases 2 and 3

Fig. 9 Axial stress of the inner tendon at the load step 1 of load case 1

5.2 Stress results

The stress results of the finite element model under load case 1 are studied in this part. Fig. 9 shows axial stress distribution of the inner tendon armor along the flexible riser. The stress at the extremities of the flexible pipe is much larger than elsewhere due to the boundary effect, which is mainly caused by the fact that constraints and forces of the model are all applied to the two extremities. Hence, the analysis of the stress within 0.1 m around the two extremities will not be included in the scope of the following analysis. The stress of tendon armor is uniformly distributed from 0.1 m~1.7 m along the flexible riser.
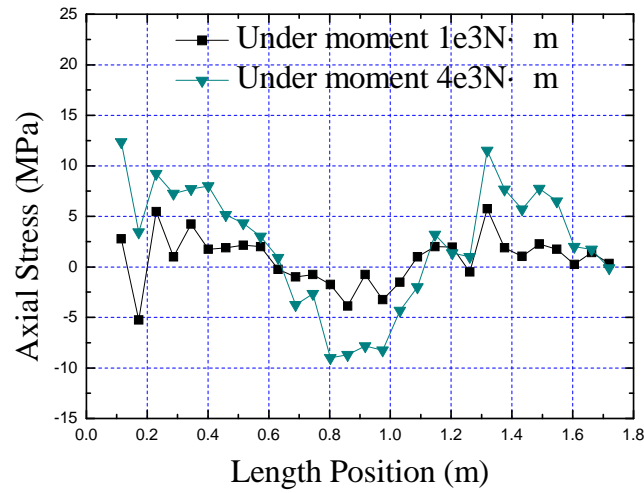
Fig. 10 Axial stress in the inner tendon at different locations in 'no-slip' state
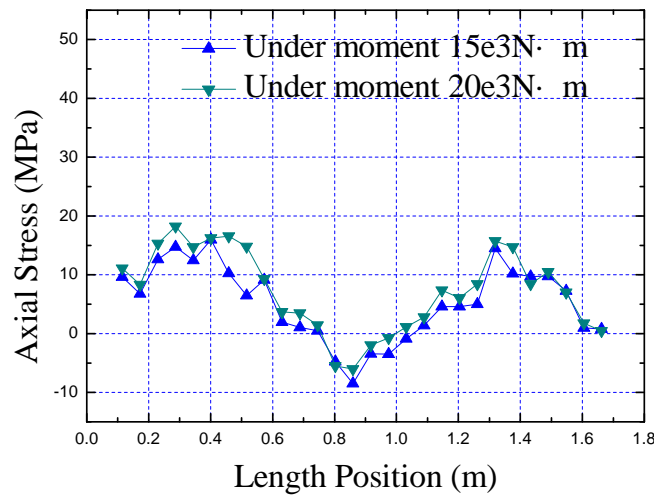

Fig. 11 Axial stress in the helical layer at different locations in sliding state

Extract the stress results of any tendon in the inner tension layer, the stress distribution of the stress along the positions of the tendon is shown in Figs.10 and 11. Since the bending response of the tendon armors are dependent upon the sliding states, bending stress analysis will be divided into the states before and after full-slipping occurs. It can be found in Fig. 5 that when the bending moment ranges from 0 to 4 kN·m, helical tendons are under no-slipping and partial-slipping states, and the tendon armors are under the full-slipping state when the bending moment exceeds 5 kN·m.

It can be noticed from Fig. 10 that the axial stress plotted in each curve changes cyclically along the length position, and almost the same trends can be found in the two lines. At a certain length position point, the axial stress increases with the enlarging of the bending moment. This indicates that in the no-slipping and partial-slipping states, positive correlation exists between the axial stress and the bending moment.

Fig. 11 reveals the relationship between the axial stress and the length position under the full-slipping state. The axial stress is in almost linear relationship with length positions and varies cyclically. Since the axial stress at this state is determined by the interlayer friction, the stress at a certain length position almost remain unchanged with the enlarging of the bending moment.

5. Conclusions

A detailed finite element model incorporating contact interaction, geometric nonlinearity, and friction has been developed to accurately simulate the structural response of the flexible riser. Based on the model, the bending moment–curvature relationships and stress of the flexible riser under bending loads together with various axisymmetric loads are studied. The results of the bending moment–curvature relationships are compared with the analytical ones obtained from the literature, good agreement has been found. The following conclusions can be derived from the analysis:

• The finite element model developed in this paper can provide an approach to predict the structural response of flexible risers under bending loads.

• When flexible risers suffer bending loads, their responses are highly nonlinear. Clear differences in the bending stiffness can be observed.

• The sliding of the tensile layer in a flexible riser is the main reason of the nonlinear bending behavior of the flexible riser. The sliding depends strongly on the contact pressure.

• Axial forces as well as internal and external pressures are the main sources of the contact pressure. Variations in axisymmetric loads can cause discrepancies in the bending responses of flexible risers.

Acknowledgments

References

Alfano, G., Bahtui, A. and Bahai, H. (2009), "Numerical derivation of constitutive models for un-bonded flexible risers", *Int. J. Mech. Sci.*, **51**(4), 295-304.
Bahtui, A., Alfano, G., Bahai , H. and Hosseini-Kordkheili, S.A. (2010), "On the multi-scale computation of un-bonded flexible risers", *Eng. Struct.*, **32**(8), 2287-2299.

Bahtuim A., Bahai, H. and Alfano, G. (2008a), "A finite element analysis for unbonded flexible risers under axial tension", *Proceedings of the 27th International Conference on Offshore Mechanics and Arctic Engineering*, Estoril, Portugal.

Bahtui, A., Bahai, H. and Alfano, G. (2008b), "A finite element analysis for unbonded flexible risers under torsion", *J. Offshore Mech. Arct.*, **130**(4), 041301.

de Sousa, J.R.M., Magluta, C., Roitman, N., Ellwanger, G.B., Lima, E.C.P. and Papaleo, A. (2009), "On the response of flexible risers to loads imposed by hydraulic collars", *Appl. Ocean Res.*, **31**, 157-170.

Do, K.D. (2011), "Global stabilization of three-dimensional flexible marine risers by boundary control", *Ocean Syst. Eng.*, **1**(2), 171-194.

Dong, L., Huang, Y., Zhang, Q. and Liu, G. (2013), "An theoretical model to predict the bending behavior of unbonded flexible risers", *J. Ship Res.*, **57**(3), 171-177.

Eom, T.S., Kim, M.H., Bae, Y.H. and Cifuentes, C. (2014), "Local dynamic buckling of FPSO steel catenary riser by coupled time-domain simulations", *Ocean Syst. Eng.*, **4**(3), 215-241.

Huang, H., Zhang, J. and Zhu, L. (2013), "Numerical model of a tensioner system and riser guide", *Ocean Syst. Eng.*, **3**(4) ,257-273.

Merino, H.E.M., Sousa, J.R.M., Magluta, C. and Roitman, N. (2010), "Numerical and experimental study of a flexible pipe under torsion", *Proceedings of the 29th International Conference on Offshore Mechanics and Arctic Engineering*, Shanghai, China.

Ren, S.F., Tang, W.Y. and Guo, J.T. (2014), "Behavior of unbonded flexible risers subject to axial tension", *China Ocean Eng.*, **28**(2), 249-258.

Saevik, S. and Berge, S. (1995), "Fatigue testing and theoretical studies of two 4 in. flexible pipes", *Eng. Struct.*, **17**(4), 276-292.

Saevik, S. and Bruaseth, S. (2005), "Theoretical and experimental studies of the axisymmetric behaviour of complex umbilical cross-sections", *Appl. Ocean Res.*, **27**(2), 97-106.

Saevik, S. and Gjosteen, J.K.O. (2012), "Strength analysis modelling of flexible umbilical members for marine structures", *J. Appl. Math.*, **2012**(985349).

Song, L.J. (2013), *The overall response characteristics research and fatigue analysis of the lazy-wave flexible riser*, Mater Dissertation, Shanghai Jiao Tong university, Shanghai, China.